applied sciences

MDPI

Article

Design of Geometrical Parameters and Kinematical Characteristics of a Non-circular Gear Transmission for Given Parameters

Silvia Maláková [1], Matej Urbanský [1], Gabriel Fedorko [2,*], Vieroslav Molnár [3] and Samuel Sivak [1]

[1] Faculty of Mechanical Engineering, Technical University of Košice, Letná 9, 042 00 Košice, Slovakia; silvia.malakova@tuke.sk (S.M.); Matej.Urbansky@tuke.sk (M.U.); samuel.sivak@tuke.sk (S.S.)
[2] Faculty of Mining, Ecology, Process Control and Geotechnologies of the Technical University of Košice, Park Komenského 14, 040 01 Kosiše, Slovakia
[3] Faculty of Manufacturing Technologies, Technical University of Kosice with a Seat in Prešov, Bayerova 1, 080 01 Prešov, Slovakia; vieroslav.molnar@tuke.sk
* Correspondence: gabriel.fedorko@tuke.sk; Tel.: +421-55-602-3143; Fax: +421-55-602-8023

Abstract: In this paper, the authors present the design of a suitable gear transmission with the continuously changing gear ratio in the range from 0.5 through 1.0 to 2.0 and back during one revolution of intermeshing gears, according to demands specified for a practical application. The gear train was designed as a pair of identical elliptical gears and the design procedure of the suitable pitch curve (ellipse) is described. The center of rotation of each of the gears is coincident with one of the pitch ellipse foci, so the gears are placed eccentrically. The gear teeth have involute profiles, but the involutes for the active and for the passive tooth sides are different. These are gears with an asymmetrical tooth profile. In the final part, the paper deals with kinematical characteristics of the designed non-circular gear transmission, which differ from the kinematical characteristics of standard circular gear transmissions with a constant gear ratio.

Keywords: design; geometrical parameters; kinematical characteristics; non-circular gear

check for updates

Citation: Maláková, S.; Urbanský, M.; Fedorko, G.; Molnár, V.; Sivak, S. Design of Geometrical Parameters and Kinematical Characteristics of a Non-circular Gear Transmission for Given Parameters. *Appl. Sci.* **2021**, *11*, 1000. https://doi.org/10.3390/app11031000

Received: 18 December 2020
Accepted: 15 January 2021
Published: 22 January 2021

Publisher's Note: MDPI stays neutral with regard to jurisdictional claims in published maps and institutional affiliations.

Copyright: © 2021 by the authors. Licensee MDPI, Basel, Switzerland. This article is an open access article distributed under the terms and conditions of the Creative Commons Attribution (CC BY) license (https://creativecommons.org/licenses/by/4.0/).

1. Introduction

Gears are one of essential components of machines and mechanisms. They are still very important elements in machine design and are irreplaceable in many cases. Gears were known and used by mankind even before the current era (BCE), mainly in the propulsion of water mills, for pumping water or lifting heavy loads. There is evidence of the knowledge in the works of Aristotle (384–322 BCE), who knew gear transmissions. The mathematician and physicist Archimedes (287–212 BCE) used gear transmissions in order to pump water (Archimedes' winch, 278 BCE). The oldest findings of gears, which were parts of the first mechanisms, include the remains of the planetarium mechanism from the first century BCE found near the island of Antikythera. A lot of gear transmissions used today were found in the schemes of Leonardo da Vinci (1452–1519) [1].

The non-circular gears were invented and designed a long time ago by predecessors of today's engineers. The first record of such a gear was a sketch by Leonardo da Vinci. Non-circular gears were mainly used in specific mechanical devices, such as clocks and toys. Later, in the 19th century, mechanical engineer Franz Reuleaux sought these types of gears to help him understand kinematics, for which he ordered a series of non-circular gear models at Gustav Voight´s "Mechanische Werkstatt" in Berlin. Back then, the gear's tooth shapes were simplified. Therefore, in all cases the meshing conditions were incorrect [2,3].

In practice, "standard" gear transmissions are used the most commonly. They can be characterized by a constant gear ratio. This means that when the drive gear rotates, the driven gear also rotates evenly, so the gear ratio has to be constant during one revolution.

The teeth of these "standard" gears have the same shape on one gear and the teeth profile is symmetrical (in exceptional cases also asymmetrical) [4].

Gear transmissions, whose gear ratio is not constant during one revolution, also find their applications in practice [5]. Such gear transmissions are used, for example:

- in flying drum shear drives as a synchronization mechanism which operates in acceleration-deceleration mode. In the period between two cuts, the blades are accelerated to the belt feed speed and decelerated again after shearing to gain time between cuts, which determines how much of the belt was fed at a given speed [6],
- in the textile industry, in order to optimize processes by improving the kinematics of machines,
- in the drives of window shade panels, in order to generate vibrations, which interfere with the natural oscillations and cancel them out [7],
- in machines for forging, for optimizing the work cycle parameters (reducing the pressure dwell time),
- non-circular gears have their application in oval gear flowmeters,
- in the automotive industry, for example in VW diesel engines, where the manufacturer reduced the load of the belt by the use of multiple atypical design elements, which also included a non-circular gearing with "nonidentical" teeth.

A non-circular transmission is the most used transmission for providing a periodically variable ratio [8]. Its advantage is that it can also provide a special motion, designed according to the equation of the motion. Nowadays, the non-circular gear set contains non-circular cylindrical gears and non-circular bevel gears with variable gear ratio [9–13]. A variable transmission ratio can also be achieved using a set of planetary gear transmissions [3].

The problem of the non-circular gear is currently devoted to several contributions. The design of non-circular gear transmission is solved in [14,15]. The design of a planetary mechanism with non-circular gear transmission is solved in [16,17]. Kinematic analysis of non-circular gears is presented in research papers [18,19]. The manufacture of non-circular gears is presented in research paper [20].

The work presented in this paper deals with the design of the geometrical model of a nonstandard eccentric elliptical gear transmission with a continuously changing gear ratio for specific parameters and with the description of its meshing, velocity and force relations.

2. Materials and Methods

2.1. Characteristics of Demands on the Gear Transmission with Changing Gear Ratio

According to demands specified by the customer for his practical application, it was necessary to create the geometrical model of a gear transmission with continuously changing gear ratio so that given transmission meets the conditions for the correct mesh of the gears. At the design of this gear transmission, the following conditions needed to be taken into consideration:

- the gear set had to be made up of two identical gears,
- the gear ratio has to change harmonically in the range from u = 0.5 through 1.0 to 2.0 and back during one revolution of the intermeshing gears,
- the number of teeth of the gears $z_1 = z_2 = 24$,
- the standardized value of the gearing module $m_n = 3.75$ mm,
- the axial distance a = 90 mm,
- the pressure angles $\alpha_n = 20^\circ$,
- intended for one sense of rotation.

In order to illustrate the issue, the customer provided also a "roughly manufactured" gear set (Figure 1). The provided gears did not meet the conditions for correct mesh.

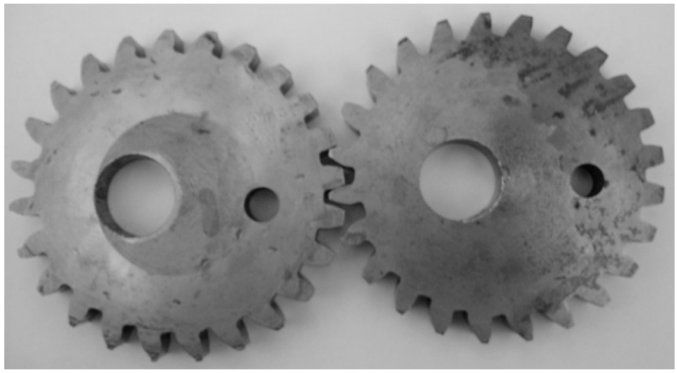


Figure 1. Model of the gear set.

2.2. Conditions of Correct Meshing of Gears

The quality of gear transmissions is determined mainly by their geometrical design [21]. In the case of an incorrect geometrical design, even the use of highest quality materials does not ensure the reliability of a gear transmission. On the contrary, the excellent geometrical design of a gearing can sometimes save the costs of an expensive material [22,23].

For the design of correctly intermeshing gears without a backlash, the essential conditions of correct meshing have to be fulfilled, according to [24,25]:

- The condition of common profile normal at each mesh point of intermeshing gears, which has to pass through the pitch point.
- The condition of mesh continuity, which means the condition of the existence of the mesh of two consecutive profiles. Providing that the pitches measured on both working circles of two intermeshing gears (for standard circular gears) are equal, this condition is fulfilled.
- The condition of the contact of teeth along the whole face width of a gearing. Providing that the helix angles on working circles are equal, this condition is fulfilled.
- The condition of circumferential velocities, which means the projections of circumferential velocities to the common profile normal have to be equal in each mesh point.
- The condition of working circle contact (the sum of the working radiuses of intermeshing gears in each mesh point equals the center distance).

The industrial standard for the involute tooth shape has been chosen for non-circular gears. Therefore, involute gearing standards and methods, which already exist, can be used and adopted [26]. Basic conditions that are required of the gearing determine the correct design for the meshing. The profiles of the teeth forming a shape bond are designed to retain a requirement for continuous meshing [27]. Transmitting of a uniform rotary motion between shafts using gear teeth, requires the normals to these teeth profiles. Every point of contact has to intersect with a virtual fixed point. For transmission of rotary motion between two shafts by gear teeth means, the instantaneous normals of the teeth profiles have to pass through a virtual fixed point [28,29].

Figure 2 represents non-circular gears like cylinders rolling together without slipping and given addendum undergone no modification. This means that nominal axle distance is applied. The gear set are depicted by the pitch curves k_1 and k_2, which have centers in the points O_1 and O_2. The pitch curve radii $r_1(\varphi)$ and $r_2(\varphi)$, which are variable, are determined for the non-circular gear set with gear ratio:

$$i(\varphi) = \frac{d\varphi}{d\psi} = \frac{1}{\psi'(\varphi)} = -\frac{r_2(\varphi)}{r_1(\varphi)} = \frac{\omega_1(\varphi)}{\omega_2(\varphi)}, \quad (1)$$

where $\omega_1(\varphi)$ and $\omega_2(\varphi)$ represent functions for the angular velocity of the gear 1 and 2.

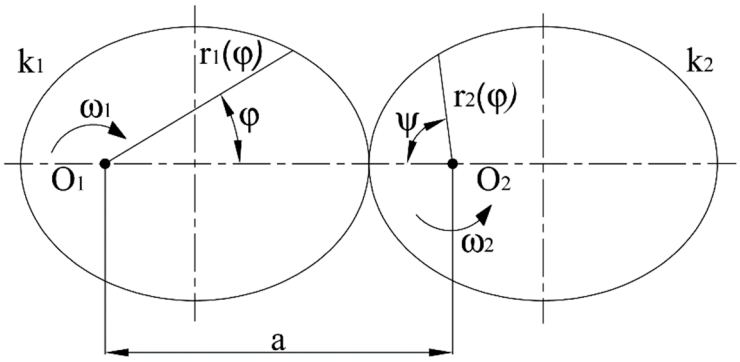


Figure 2. Example of non-circular pitch curves.

Equation for the center distance is the following:

$$a = \text{constant} = r_1(\varphi) + r_2(\varphi), \tag{2}$$

where $\psi'(\varphi)$ is the transmission function, which describes pitch curves of the non-circular gear set relation.

2.3. Velocity Relations in Ideal Intermeshing Spur Gears

Standard (circular) spur gears perform a rotary motion of angular velocities $\omega_{1,2}$ about their axes of rotation. Individual points of gears move in circular paths at the circumferential velocity, which is determined in the central point of mesh *C* by the distance of pitch radii $r_{1,2}$ according to the equation [30]:

$$v = v_1 = v_2 = r_1^X * \omega_1 = -r_2^X * \omega_2, \tag{3}$$

where $r_1{}^X$ and $r_2{}^X$ represents connecting lines of the point *X* to the centers of rotation O_1 and O_2 (Figure 3).

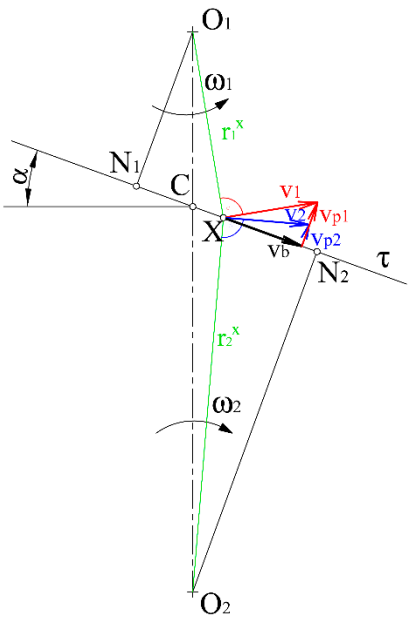


Figure 3. Velocity relations in intermeshing spur gears.

The circumferential velocity of intermeshing gears is an important indicator in the velocity relations. Depending on the circumferential speed (v), gears can be divided into

three groups: low-speed gears ($v \leq 5$ m.s^{-1}); medium speed gears (5 m.s^{-1} < v < 20 m.s^{-1}) and high-speed gears ($v \geq 20$ m.s^{-1}) [31].

In any mesh point *X* on the line of action τ, the circumferential velocity of the point of contact of the driver (with the center of rotation in the point O_1) is v_1 and the circumferential velocity of the point of contact of the driven gear (with the center of rotation in the point O_2) is v_2 (Figure 3). The directions of these velocities are perpendicular to the connecting lines $r_1{}^X$ r1X and $r_2{}^X$ of the point X to the centers of rotation O_1 and O_2.

In the transverse plane, the velocities v_1 and v_2 can be decomposed into two perpendicular components, according to the equations:

$$\vec{v}_1 = \vec{v}_b + \vec{v}_{p1} \text{ and } \vec{v}_2 = \vec{v}_b + \vec{v}_{p2} \quad (4)$$

The velocities v_{p1} and v_{p2} are sliding velocities. They are situated on the common tangent to the profiles of both gears and are perpendicular to the line of action. The velocity v_b is a driving velocity. It is situated on the line of action τ and it is the velocity of the point X, which is moving in the path of action (in the straight line τ).

From the condition of the continuous contact of the profiles of both teeth in any point X on the line of action, it follows that the driving velocity v_b of both intermeshing gears has to be equal.

The sliding velocities v_{p1} and v_{p2} are not equal and their vector subtraction equals the relative velocity of the instantaneous mesh point v_s:

$$v_{s21} = v_2 - v_1 = v_{p2} - v_{p1} = -v_{s12} \quad (5)$$

The velocities v_1 and v_2 are circumferential velocities on the radii $r_{1,2}{}^X$ and their magnitude is given by Equation (3). The velocity v_b follows from velocity triangles and using Equation (3) we acquire:

$$v_b = v_1 * \cos \alpha_1^X = v_2 * \cos \alpha_2^X = r_{b1} * \omega_1 = -r_{b2} * \omega_2 \quad (6)$$

The velocities v_{p1} and v_{p2} follow from velocity triangles:

$$v_{p1} = v_1 * \sin \alpha_1^X = r_1^X * \sin \alpha_1^X = \rho_1 * \omega_1 \quad (7)$$

$$v_{p2} = v_2 * \sin \alpha_2^X = -r_2^X * \sin \alpha_2^X = -\rho_2 * \omega_2, \quad (8)$$

where $\rho_{1,2}$ are the radii of curvature in the mesh point X. In Equation (7) are the minus signs in order to the corresponding velocities were positive with regard to the sense of $r_2{}^X$ and ω_2.

That means that the projections of the circumferential velocities v_1 and v_2 in any point of mesh onto the common normal have to be equal, while the circumferential velocities consist of the driving velocity v_b and the sliding velocities v_{p1} a v_{p2}, which lie on the common tangent to the profiles of both gears and thus perpendicular to the line of action.

3. Results and Discussion

3.1. Design of the Pitch Curve Shape

These non-circular gear sets were developed considering the law of motion of the driven gear, for variable gear ratio and the elliptical shape of pitch curve of the driving gear wheel [32].

The first step in a gearing design is the design of a pitch curve. Regarding "standard" gears, the pitch curve is created by a pitch circle with the center situated on the axis of rotation.

Based on the results of the solution of the given problem using gears with circular shape and eccentrically placed centers of rotation, the elliptical shape of the gears was chosen. The geometrical gear wheel center is not same as the rotation center of this gear

wheel. The center of rotation of the gear was chosen in the focus of the ellipse. The dimensions of the chosen pitch ellipse of the gear are visible in Figure 4.

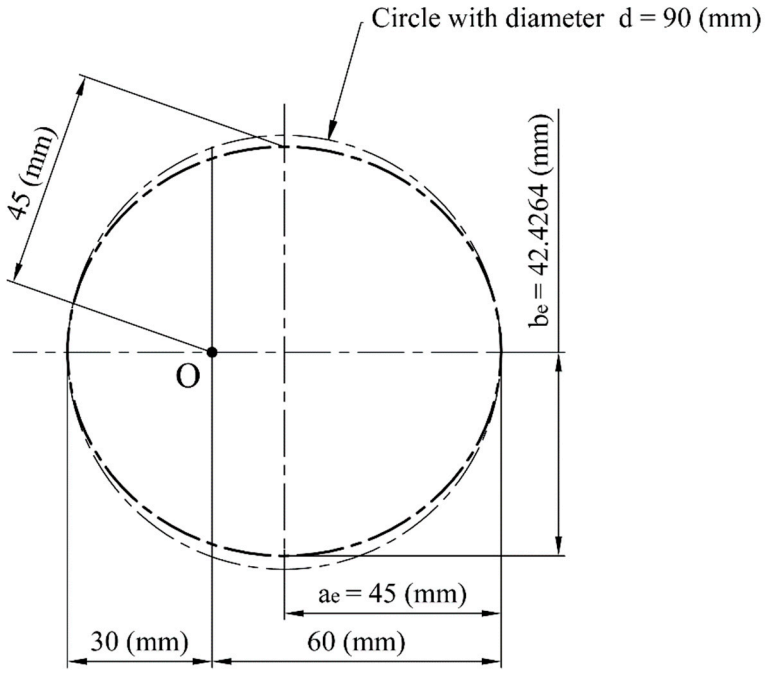


Figure 4. Dimensions of the designed pitch ellipse.

The length of the semimajor axis of the pitch ellipse a_e = 45 mm was computed from the given axial distance a = 90 mm. The centers of rotation of the gears O_1 and O_2 were determined according to the demand to create a transmission with the time-variable gear ratio in the range from 0.5 through 1.0 up to 2.0. When $r_1 + r_2 = 90$ mm, where $r_1 = r_2$ and $r_2 / r_1 = 1.0$, the gear ratio equals 1.0 and the length of the semiminor axis of the ellipse b_e can be determined: b_e = 42.426 mm (Figure 4). The points O_1 and O_2 are the foci of the pitch ellipses as well. According to the property of an ellipse, which is true for each point X of the ellipse, the sum of the distances O_1X and O_2X equals the twice the length of the semimajor axis, in this case the sum equals the axial distance.

In Figure 5, the pitch ellipses of the eccentrically placed intermeshing elliptical gears and also the pitch ellipse division into 24 pitches (according to the number of teeth z = 24), which are equal in length, are shown. Both gears are identical, therefore the same marking of teeth was chosen on both intermeshing gears. The rotational speed of the driving elliptical gear wheel has the symbol n_1 in the Figure 5, n_2 is the rotational speed of the driven wheel.

There are values of pitch radii and values of variable gear ratio for designed elliptical gear set in Table 1.

In Table 1 are the values of pitch radii, in particular mesh points, denoted by the symbols $r_{1\text{-}i}$ or $r_{2\text{-}j}$ where the index 1 stands for the driving gear, index 2 for the driven gear, index i, or j is the order number of the mating tooth (Figure 5) at one revolution of the driving and driven gear. This table shows the variable gear ratio of the intermeshing gears as well, in the range from 0.5 (the first pair of teeth mates, the tooth 24 of the driving gear is in mesh with the tooth 12 of the driven gear) through the gear ratio = 1.0 (if the tooth 6 of the driving gear is in mesh with the tooth 6 of the driven gear), up to the gear ratio = 2.0 (if the tooth 12 of the driving gear is in mesh with the tooth 24 of the driven gear) and back through the gear ratio = 1.0 to the gear ratio = 0.5.

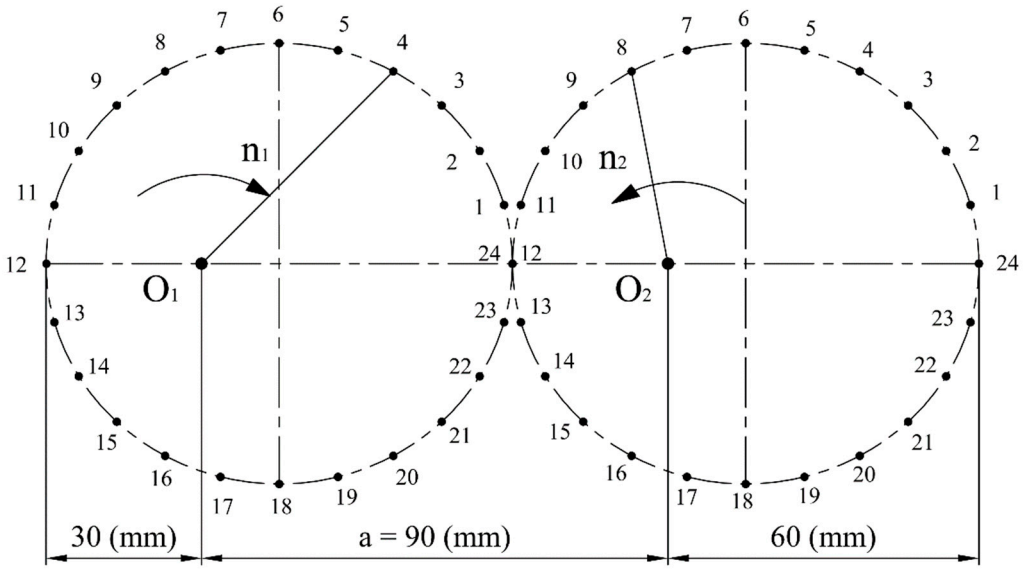


Figure 5. Pitch ellipses of the eccentrically placed intermeshing gears.

Table 1. Pitch radii and changing gear ratio.

Tooth of Driving Gear—Order Number	Pitch Radius $r_{1\text{-}i}$ (mm)	Tooth of Driven Gear—Order Number	Pitch Radius $r_{2\text{-}j}$ (mm)	Gear Ratio $u_i = r_{2\text{-}j}/r_{1\text{-}i}$	Axial Distance $r_{1\text{-}I} + r_{2\text{-}j}$ (mm)
24	60	12	30	0.5	90
01	59.458972	11	30.541025	0.5136	90
02	57.891981	10	32.108009	0.5546	90
03	55.449504	09	34.550498	0.6230	90
04	52.336954	08	37.663046	0.7196	90
05	48.778898	07	41.221102	0.8450	90
06	45	06	45	1	90
07	41.221102	05	48.778898	1.1833	90
08	37.663046	04	52.336954	1.3896	90
09	34.550498	03	55.449504	1.6048	90
10	32.108009	02	57.891981	1.8030	90
11	30.541025	01	59.458972	1.9468	90
12	30	24	60	2	90
13	30.541025	23	59.458972	1.9468	90
14	32.108009	22	57.891981	1.8030	90
15	34.550498	21	55.449504	1.6048	90
16	37.663046	20	52.336954	1.3896	90
17	41.221102	19	48.778898	1.1833	90
18	45	18	45	1	90
19	48.778898	17	41.221102	0.8450	90
20	52.336954	16	37.663046	0.7196	90
21	55.449504	15	34.550498	0.6230	90
22	57.891981	14	32.108009	0.5546	90
23	59.458972	13	30.541025	0.5136	90

For each tooth, the pitch ellipse has to meet the condition that the sum of radii equals the axial distance:

$$r_{1-i} + r_{2-j} = a = 90\text{mm} \tag{9}$$

The pitch ellipse is given by the parametric equations (φ is the eccentric anomaly of an ellipse $\varphi \in 0, 2\pi$) [33]:

$$\begin{aligned} x &= a_e * \cos\varphi \\ y &= b_e * \sin\varphi \end{aligned} \tag{10}$$

The length of the semimajor axis of the ellipse is a_e = 45 mm, which is the half of the axial distance. The length of the semiminor axis is determined by the distance of 45 mm from the focus (Figure 3), which position was determined considering the needed gear ratio. The length of the semiminor axis was computed according to the formula:

$$b_e = \sqrt{a_e^2 - (a_e - 30)^2} = 42.426407\text{mm} \quad (11)$$

The numerical eccentricity of the ellipse [34]:

$$\frac{\sqrt{a_e^2 - b_e^2}}{a_e} = 0.3333\text{mm}, \quad (12)$$

where a_e—semimajor axis of the ellipse (mm), b_e—semiminor axis of the ellipse (mm).

3.2. Creation of the Geometrical Model of the Elliptical Gear Set

The tooth side profile curve consists of two portions, the involute and the non-involute portion. Only the involute portion of the tooth profile is allowed to be active during meshing of a gear [35]. The function of the non-involute portion of the tooth profile is to create a smooth rounded transition between the involute portion of the toothing and the root cylinder.

In general, an involute is created as the trajectory of a point on a piece of taut string as the string is unwrapped from a curve. The geometrical locus of the curvature centers of an involute is called evolute (Figure 6).

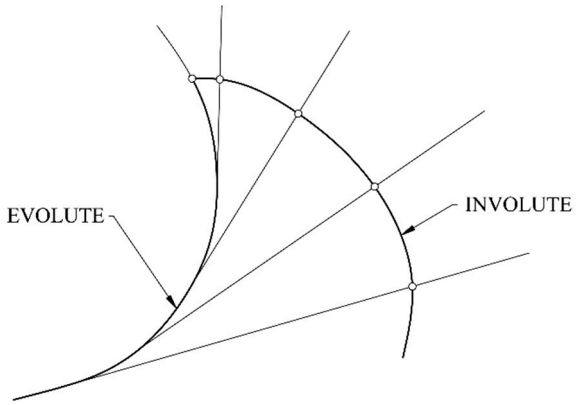


Figure 6. Involute, evolute.

Regarding standard involute gears, in order to create the teeth profiles the involute is used, of which the evolute is a circle. Therefore, the created straight line is the normal of the involute and also the tangent to the base circle (evolute) with the point of contact in the curvature center of the involute. In this case, the involute is unambiguously determined by one parameter, namely the base circle radius.

In the first solution, the involute was created by rolling the created straight line on the base circle despite fact that in this case we dealt with elliptical gears. The center of the base circle was always coincident with the center of rotation in the eccentrically placed gear. It means that an involute was created by each central point of rolling. The involute was created by rolling the created straight line on the base circle of variable diameter according to the relation:

$$d_{bi} = d_i * \cos \alpha_n \quad (13)$$

where d_i is the pitch circle size for individual teeth and the pressure angle in the normal plane $\alpha_n = 20^\circ$ (Figure 7). For the drawing of the involute portion of the tooth side profile, the trochoidal method of involute construction was used.

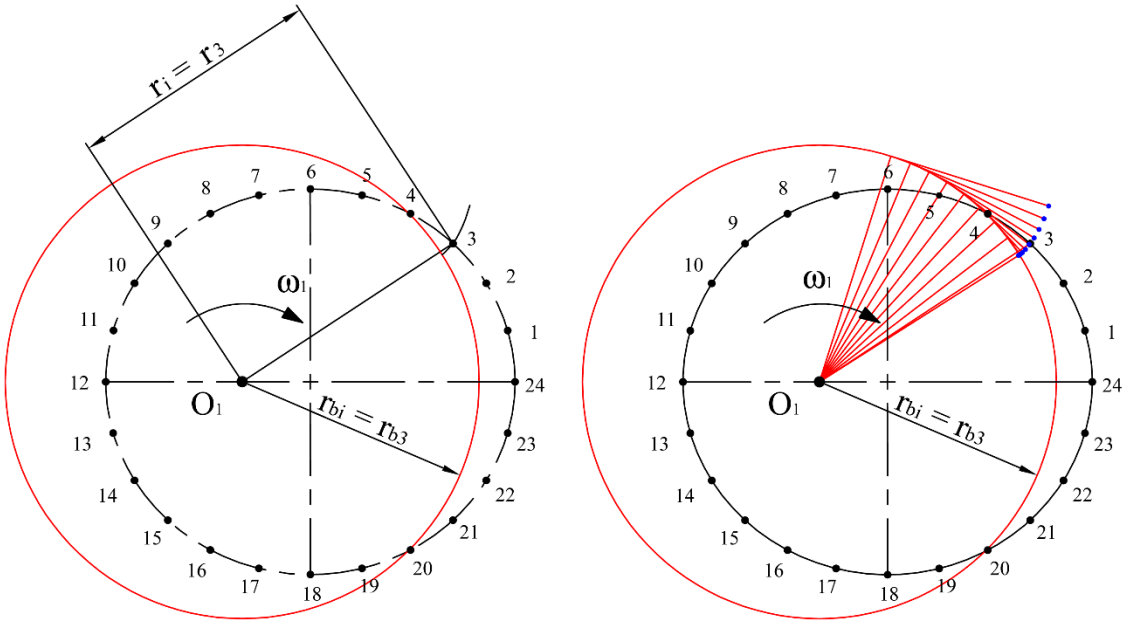


Figure 7. Example of involute construction from base circle for the tooth with order number 3.

The diameters of the base circles for the left and the right side of a tooth are different. The resulting shape of the gear created this way is shown in Figure 8a and it is identical with the shape of the model provided by the customer. These gears are not functional (Figure 8b), because the teeth interfere and the conditions of correct meshing are not met.

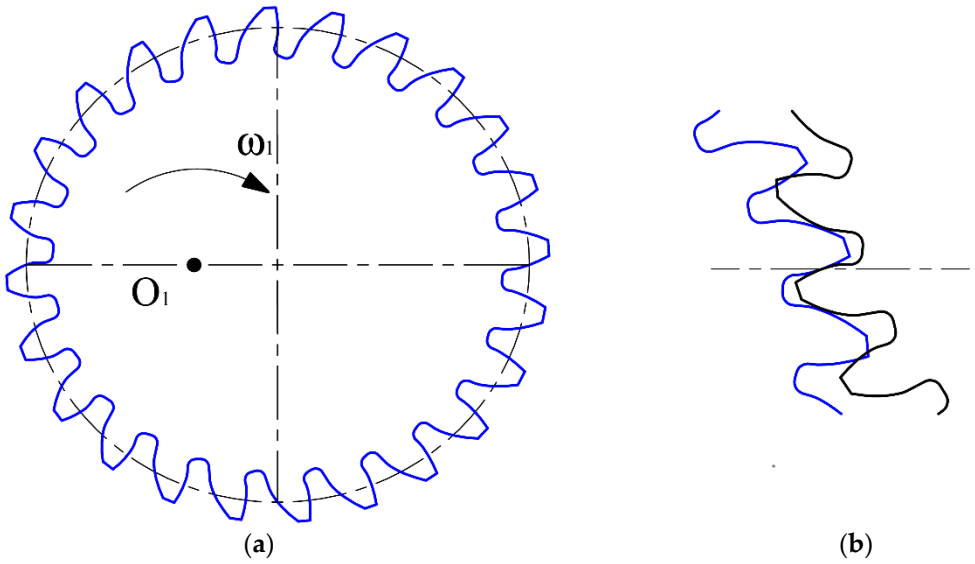


Figure 8. (**a**) Resulting shape of the gear; (**b**) the teeth interfere—the conditions of correct meshing are not met.

Based on this finding, a more accurate tooth design was needed, so the involute portion of the tooth side profile was created by rolling the tangent on the base ellipse as the trajectory of a point. For this solution, the first step of constructing the involute portion of the teeth side profiles was the construction of tangents in the central points of contact on the pitch ellipse.

In order to create the tangents, a separate construction was used (Figure 9). In Figure 9, the construction of the normal (denoted by the letter n) and the tangent (denoted by the letter t) for the active side of the tooth denoted by the number 4 in the central point of mesh of this tooth, so the construction of the normal and tangent to the pitch ellipse is shown.

The points 1p, 2p, 3p, etc., marked in red are the points for the passive sides of individual teeth. The center of rotation of the gear is denoted by the letter O. This center is also one of the foci—F_1 of the pitch ellipse. The second focus of the pitch ellipse is denoted by the symbol F_2.

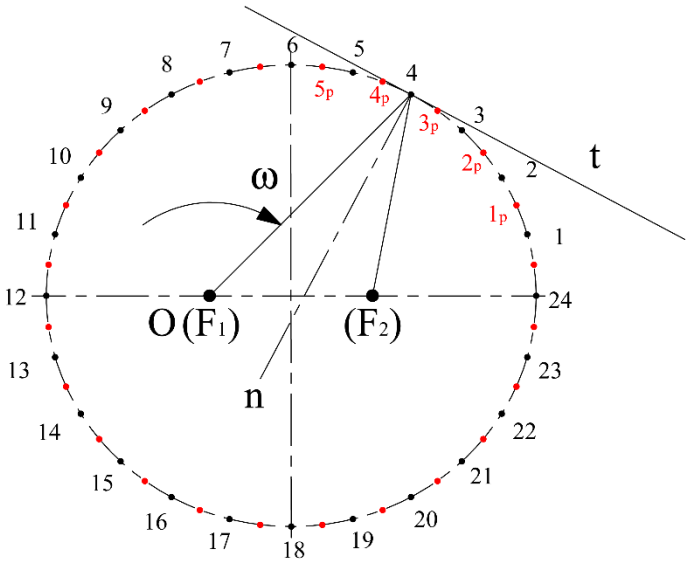


Figure 9. Construction of the tangent "*t*" and normal "*n*" to the pitch ellipse.

The second step was the determination of the evolute of the involute, so the geometrical locus of the points N_i as the last points of mesh (Figure 10).

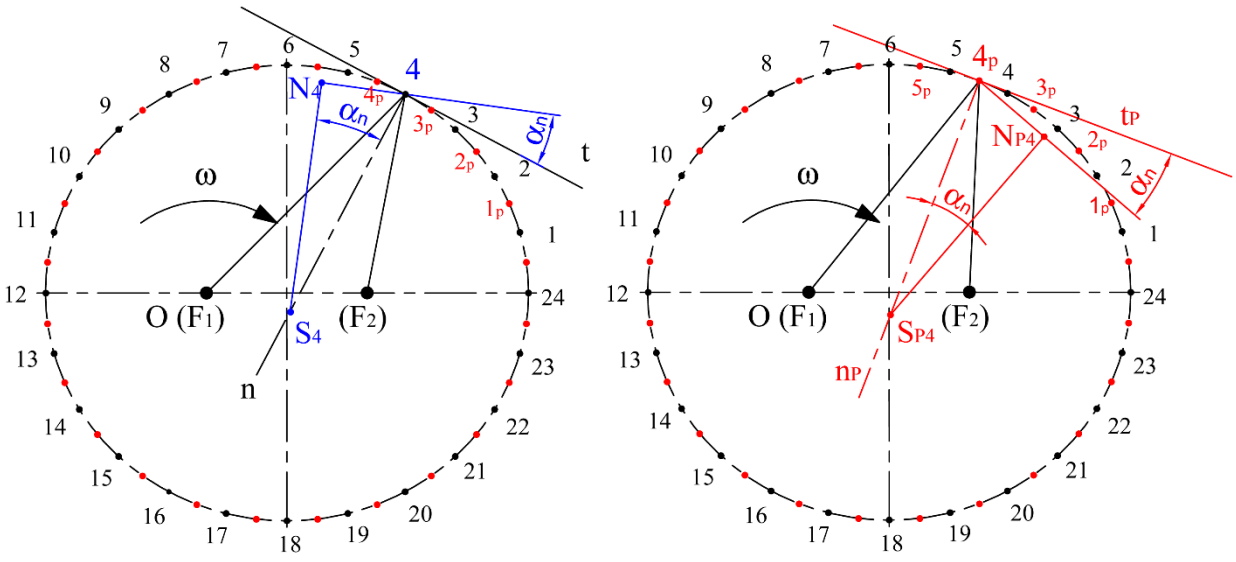


Figure 10. Construction of the last points of mesh N_i.

Therefore, it was necessary to construct straight lines tilted at the pressure angle α_n = 20° in the central point of mesh for each tooth individually and to determine the position of the involute curvature centers S_i and S_{pi} (for the left and also right side of each tooth). The curvature centers of the ellipse lie on the normal and they are determined by the curvature centers r_{ie}.

$$r_{ie} = \frac{1}{a_e^4 b_e^4}\sqrt{\left(a_e^4 y_i^2 + b_e^4 x_i^2\right)^3} \tag{14}$$

where x_i, y_i are the coordinates of a point on the pitch ellipse. The left and the right side of each tooth were solved individually. The points N_i for the right sides of the teeth determine the evolute. The points N_{pi} determine the second evolute for the left sides of the teeth. Figure 10 illustrates the construction of the evolutes for the left and right side of the tooth number 4.

In Figure 11 is the trochoidal method of construction of the involute curve of the tooth side profile if the evolute of the involute is the ellipsis.

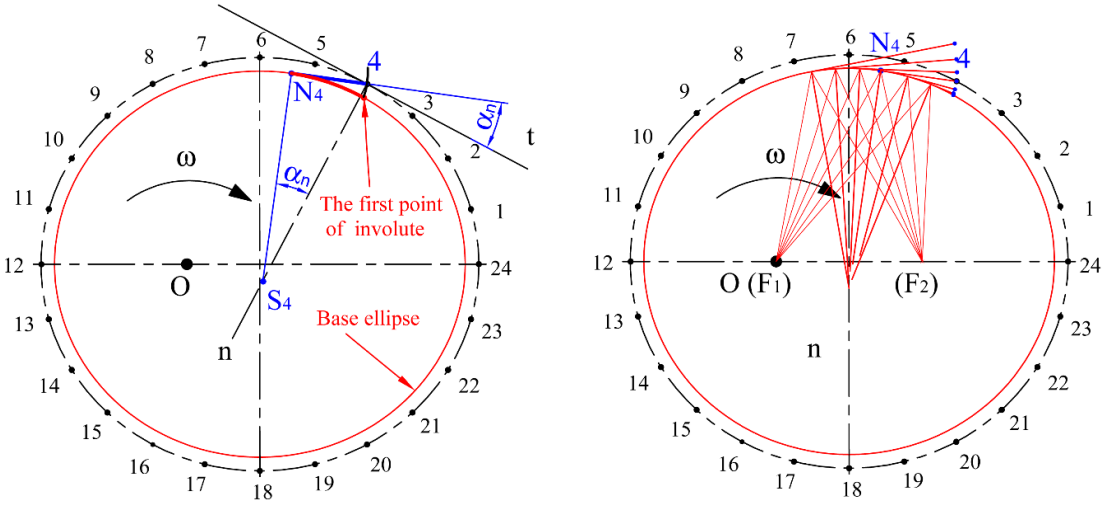


Figure 11. Example of involute construction from base ellipse for the tooth with number 4.

Using the trochoidal method of involute construction (Figure 11), the points of the involute for each side of a tooth were laboriously created. The more involute points are created using the above described trochoidal method, the more accurate the shape of the involute portion of the tooth side profile we acquire.

The difference in the construction of these tooth profiles from the reference [36] is in the formation of the active curve of the tooth profile. The methods of involute construction used in the references used the base circle as the evolute. The procedure described in this article is different. The evolute has the shape of a (basic) ellipse (Figure 11). The difference in the procedure is also visible in the position—the location of the wheel teeth with respect to the center of rotation. The principal difference between the shape of teeth due to the differential creation of the involute is in Figure 12.

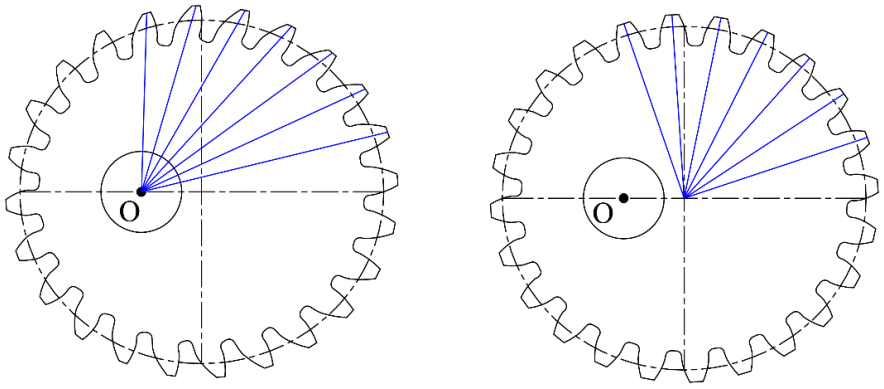


Figure 12. Principal difference between the shape of teeth due to the differential creation of the involute.

A root transition is the surface between the involute surface of a tooth and the root cylinder. The function of the non-involute portion of the profile of a tooth is to create a

smooth transition between the involute portion of the toothing and the root cylinder. It is a very important region, because it determines considerably the flexural strength and the interference phenomena during meshing [37]. The shape of the non-involute portion of the profile of a tooth depends on the manufacturing method of the toothing. The manufacture of a toothing by a rack cutter is one of the most used manufacturing methods, where the non-involute portion of the tooth side profile is the envelope of the positions of the rack cutter which rolls on the pitch circle of a gear. Such creation of the non-involute portion of the tooth side profile is not suitable for the given elliptical eccentrically placed gear. For the geometrical design, the following formula for computing the fillet radius of the non-involute portion of the tooth side profile was used [38]:

$$r_f = 0.38m_n \tag{15}$$

where m_n is the module in the normal plane. For spur gears (with straight teeth), the value of m_n equals the value of the module in the transversal plane, $m_n = m_t = m$. Non-involute portions of the tooth profile (its left and right side) were constructed using the same fillet radius $r_f = 1.425$ mm.

By connecting the involute and the non-involute portion of a tooth side profile we create one tooth side profile. In order to create one complete tooth profile, we need further inputs such as the dimensions of the tip and root cylinders (for circular gears) which create the height boundaries of the tooth. In the case of the created model of the elliptical gear set with eccentrically placed centers, the dedendum is determined by the pitch ellipse offset in the distance of 1.25 times of the module value in the normal plane (Figure 13). The addendum does not equal the module, because the involute and the non-involute portion of the tooth side profile would be in mesh. The addendum has to be reduced so that the correct mesh of the intermeshing gears occurs.

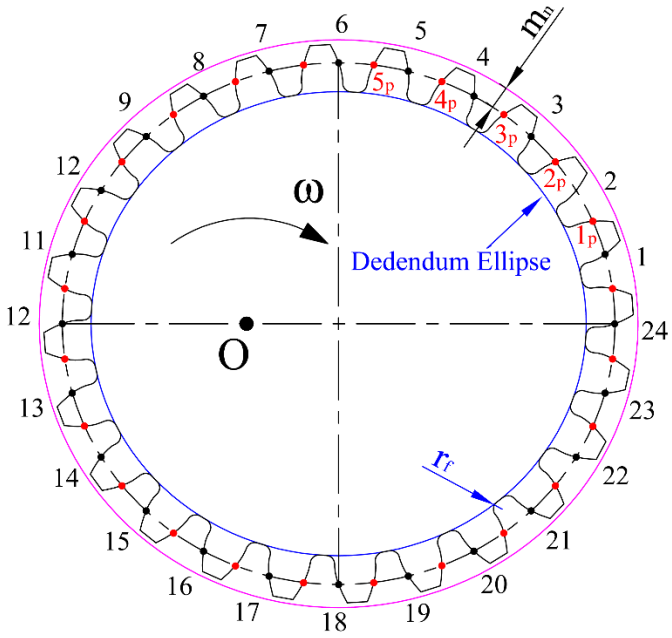


Figure 13. Resulting shape of the gear toothing.

Based on the tooth contact analysis, it was necessary to adjust the height of the addendum. Three-dimensional contact analysis in SolidWords was used. The reduction in height of addendum is shown in Figure 14. The design of parameters for gear dimensions was based on the modulus value $m_n = 3.75$ mm. This module was specified by the customer. The tooth dedendum is $h_f = 1.25m_n$. The addendum of the tooth was modified, its value was reduced from value $h_a = m_n = 3.75$ mm to value $h_a = 3$ mm.

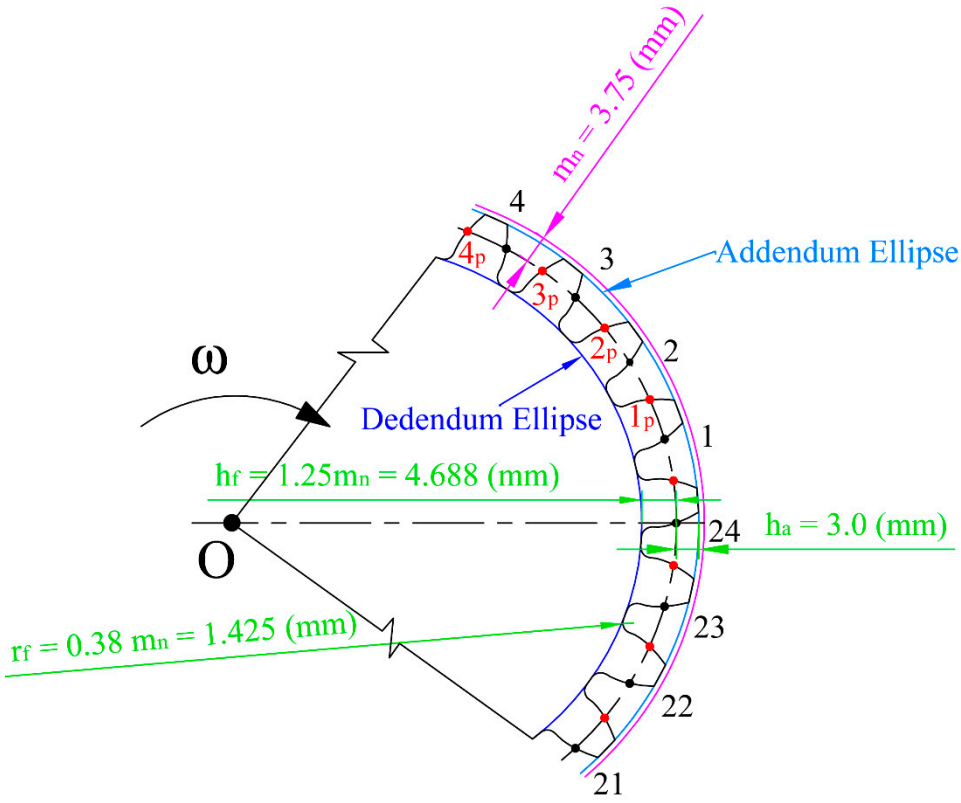


Figure 14. Dedendum and addendum of teeth.

The difference between the tooth profile of the designed elliptical gear set and the tooth profile of the standard spur gear is shown in Figure 15. The profile of spur gear tooth with the number of teeth z = 24 and the module $m_n = m_t = m = 3.75$ mm is drawn using black color. The profile of the tooth denoted by the number 6 in the central point of mesh (Figure 5) is drawn using red color. At the mesh of the tooth with the intermeshing gear, the gear ratio u = 1 of the designed elliptical gear set is achieved.

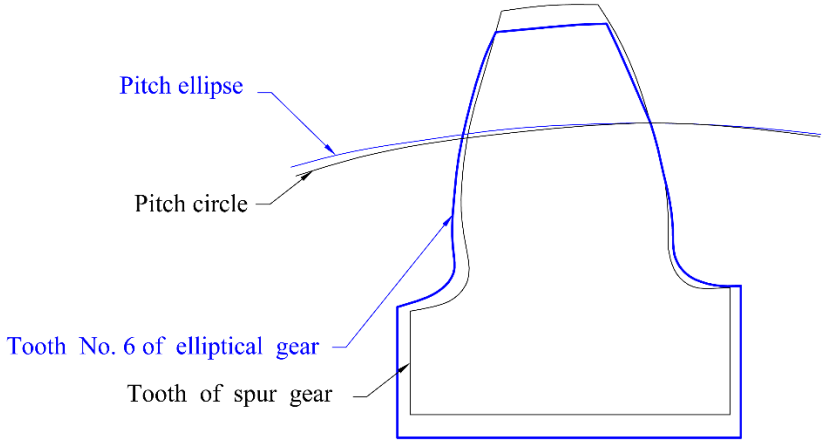


Figure 15. Tooth profile comparison for tooth No. 6.

Standard spur teeth are teeth with a symmetrical profile. Left and right active—involute curve has the same shape. The teeth of the designed non-circular gear have an asymmetrical tooth profile. The left involute curve of the tooth profile is different from the right. In Figure 16 is an example of the difference for the left and right side of tooth

number 6 of the proposed gear. It is the result of different evolutes of involute tooth curves (Figure 10).

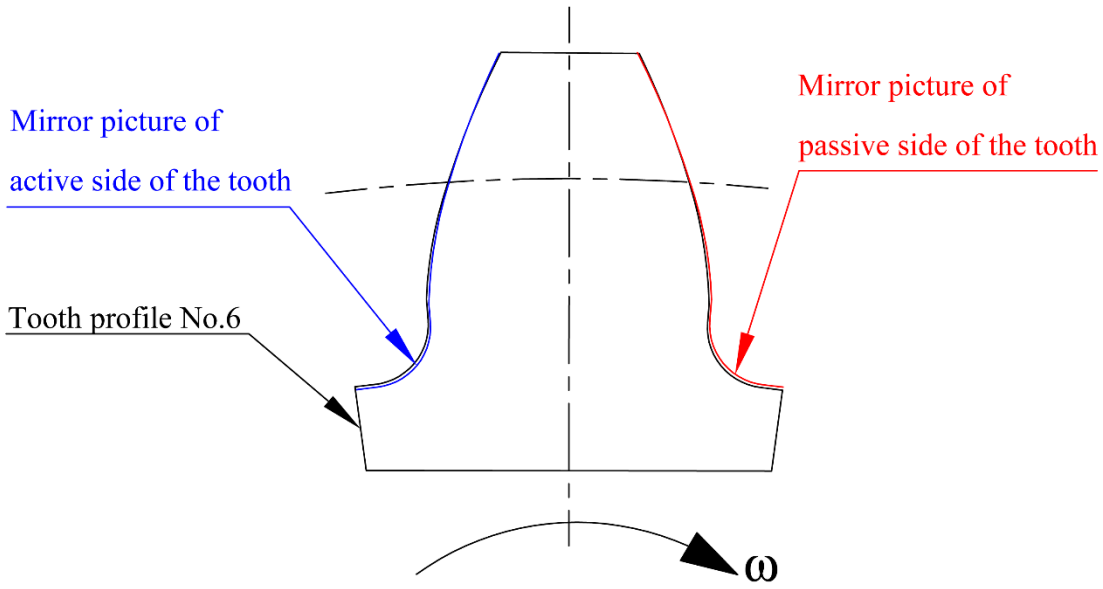


Figure 16. Asymmetry of tooth No. 6.

The gears for the given transmission with the time-variable gear ratio were designed as elliptical gears which were eccentrically placed so that the conditions of correct mesh were met (Figure 17).

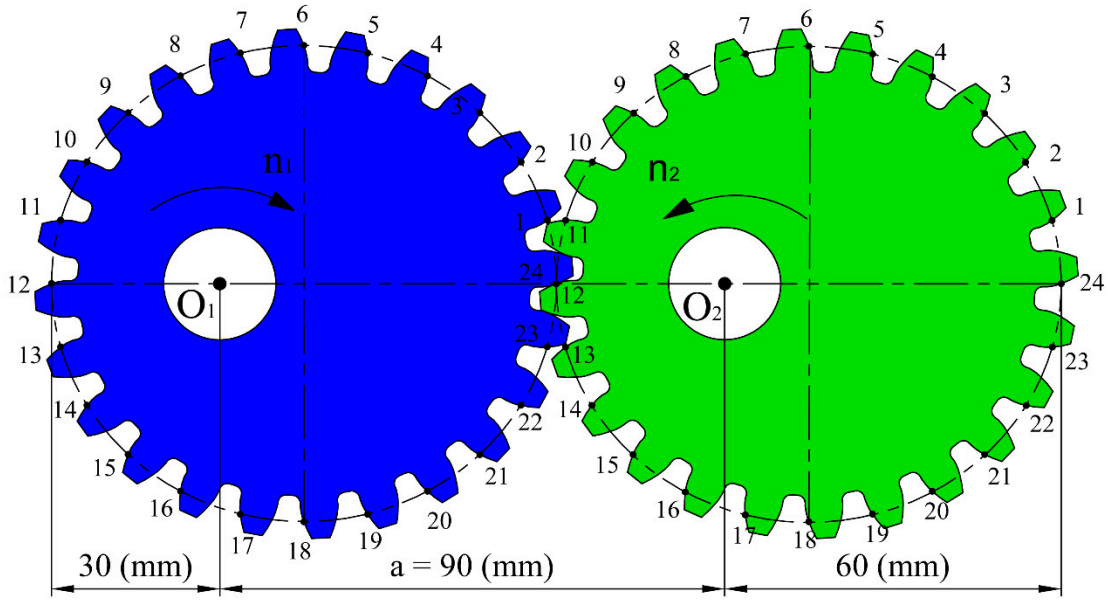


Figure 17. Designed model of elliptical gear set.

3.3. Velocity Relations in the Designed Elliptical Gear Set

When researching the kinematics of the designed gear set with eccentrically chosen centers of rotation, we followed the condition of a correct mesh, which defined that circumferential velocities in the central point of mesh are equal and their projections to the profile normal are equal. Studied kinematical parameters are processed for the driving elliptical gear—index 1 (with the center of rotation in the point O_1) and for the driven elliptical gear—index 2 (with the center of rotation in the point O_2). The graphical

representation of kinematical dependences of both gears is chosen in a single graph (on the horizontal axis are the driving gear teeth—z_1). For solving the given issue, the constant angular velocity of the driving elliptical gear, $\omega_1 = 100\ s^{-1}$ was chosen.

In Figure 18, the courses of angular velocity of the driving ($\omega_1 = 100\ s^{-1}$) and the driven (ω_{2i}) elliptical gear are shown. Unlike standard circular gears, where the angular velocity of the driving and also of the driven gear is constant, in this case, the angular velocity of the driven eccentrically placed gear is not constant, but it varies depending on the continuously changing gear ratio (Figure 19). For example, if the teeth are meshing where a gear ratio of 0.5 is achieved (tooth number 24 on the driving wheel and tooth number 12 on the driven wheel), at that moment the angular velocity of driving wheel has the value $\omega_1 = 100\ s^{-1}$, but on the driven wheel there is an angular velocity $\omega_2 = 200\ s^{-1}$. These values apply if the point of teeth contact is at the pitch point. When tooth number 6 on the driving wheel is meshing with tooth number 6 on the driven wheel, the angular velocity is the same for both the driving wheel and the driven wheel ($\omega_1 = \omega_2 = 100\ s^{-1}$). The angular velocity of the driving wheel is constant, ω_1 = const. The angular velocity of the driven wheel is not constant, it depends on the changing gear ratio, $\omega_2 = f(u)$.

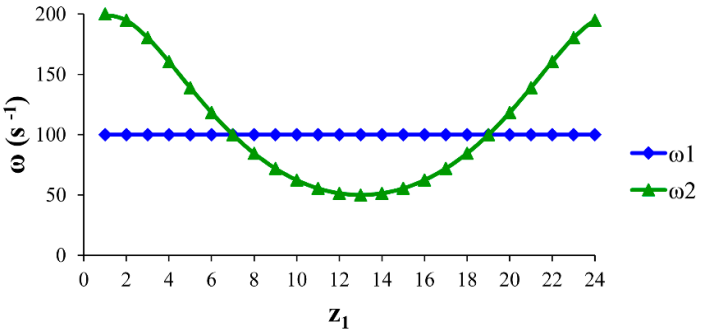


Figure 18. The course of angular velocities in the designed elliptical gear set.

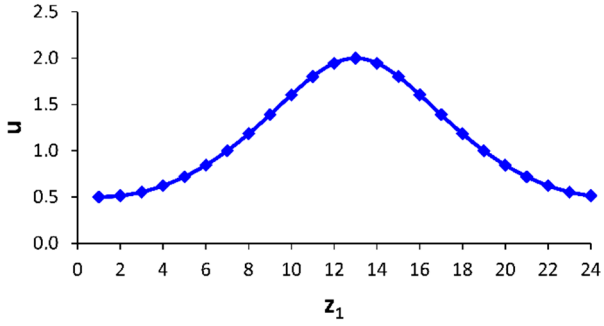


Figure 19. The course of changing gear ratio in the designed elliptical gear set.

Simultaneously, it follows from Figure 20 that the gear ratio of the designed, eccentrically placed elliptical gear transmission depends on the angle of rotation φ of the driving gear (Figure 21) and thus the gear ratio of the designed gear transmission is the function of this angle of rotation:

$$u = f(\varphi) \tag{16}$$

Figure 22 shows the length of part of contact of tooth number 24 of the driving wheel with tooth number 12 of the driven wheel. The point A is the first point of meshing of tooth number 24 of driving wheel. The point E is the last point of meshing of tooth number 24 of the driving wheel. The change of the gear ratio was investigated for this tooth—see Figure 23.

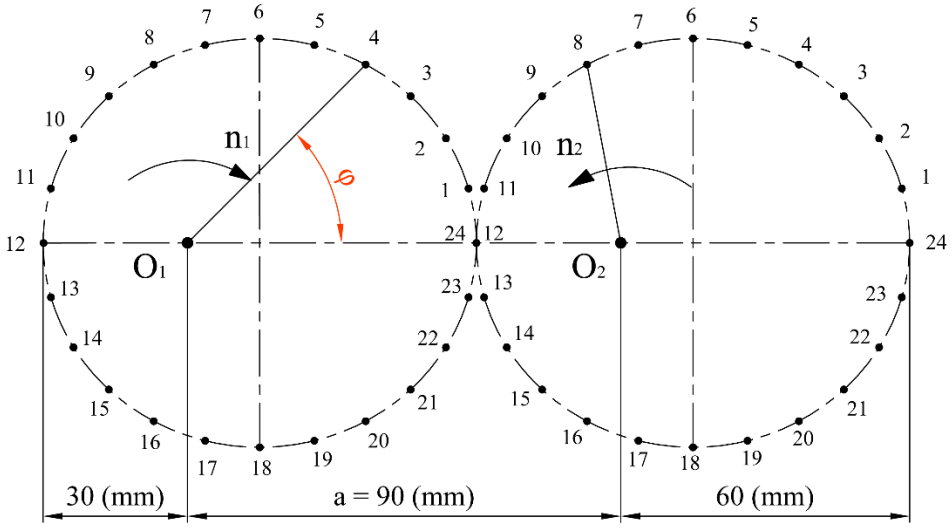


Figure 20. Defining the angle of rotation of the driving gear.

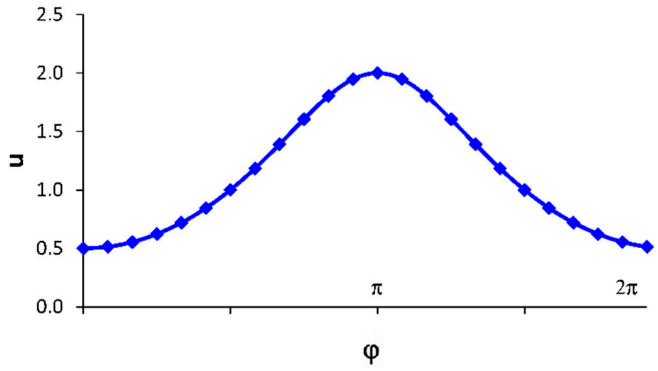


Figure 21. The course of the gear ratio dependent on the angle of rotation of the driving gear.

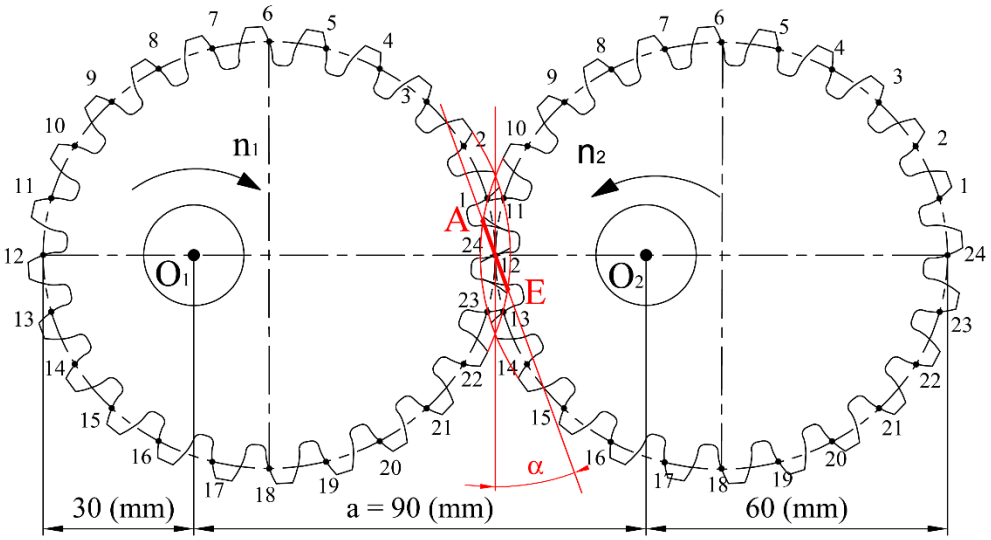


Figure 22. The length of part of contact.

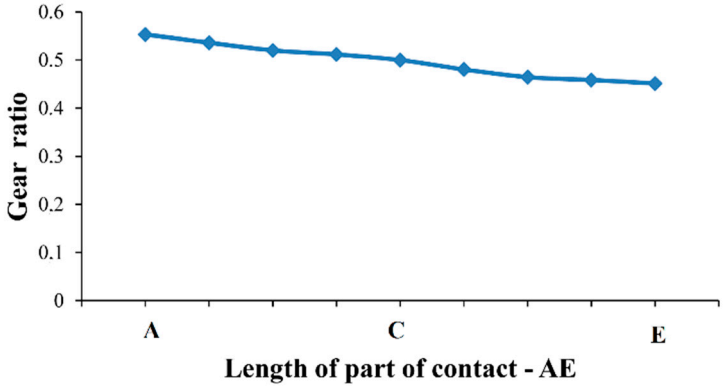


Figure 23. The course of changing gear ratio of the meshing teeth pair, driving wheel tooth number 24 and drive wheel tooth number 12.

The standard spur gears have the constant (same) contact ratio for all teeth of meshing. The value of the contact ratio (CR) of meshing for spur gears is in the range $1 < CR < 2$. This is not the case with the designed elliptical gearing. The values of length of meshing line AE and contact ratio for elliptical and spur gearing are shown in Table 2 and Figure 24.

Table 2. Length of part of contact *AE* and contact ratio.

Elliptical Gearing		Gear Ratio $u_i = r_{-j}/r_{1-i}$	Spur Gearing (m_n = 3.75 mm)			
AE (mm)	*CR*		Pitch Radius r_{1-i} (mm)	Pitch Radius r_{2-j} (mm)	AE (mm)	CR
14.482	1.3081	0.5	60	30	17.527	1.5832
14.494	1.3092	0.5136	59.458	30.541	17.542	1.5845
14.526	1.3122	0.5546	57.891	32.108	17.583	1.5883
14.568	1.3159	0.6230	55.449	34.550	17.636	1.5931
14.607	1.3195	0.7196	52.338	37.663	17.686	1.5976
14.634	1.3219	0.8450	48.779	41.221	17.721	1.6001
14.644	1.3228	1.0	45	45	17.733	1.6002
14.634	1.3219	1.1833	41.221	48.779	17.721	1.6001
14.607	1.3195	1.3896	37.663	52.338	17.686	1.5976
14.568	1.3159	1.6049	34.550	55.449	17.636	1.5931
14.526	1.3122	1.8030	32.108	57.891	17.583	1.5883
14.494	1.3092	2.0	30.541	59.458	17.542	1.5845

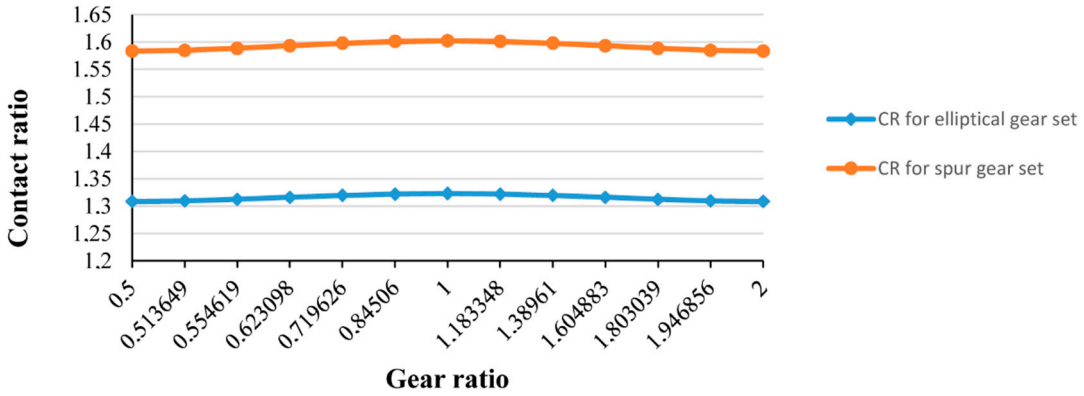


Figure 24. The course of contact ratio for elliptical and spur gear sets.

To compare the difference in the change of the contact ratio, the value of the contact ratio for a pair of teeth with a gear ratio equal to 1 (u = 1) was chosen as the basis. Figure 25 shows a comparison of the change in the contact ratio parameter.

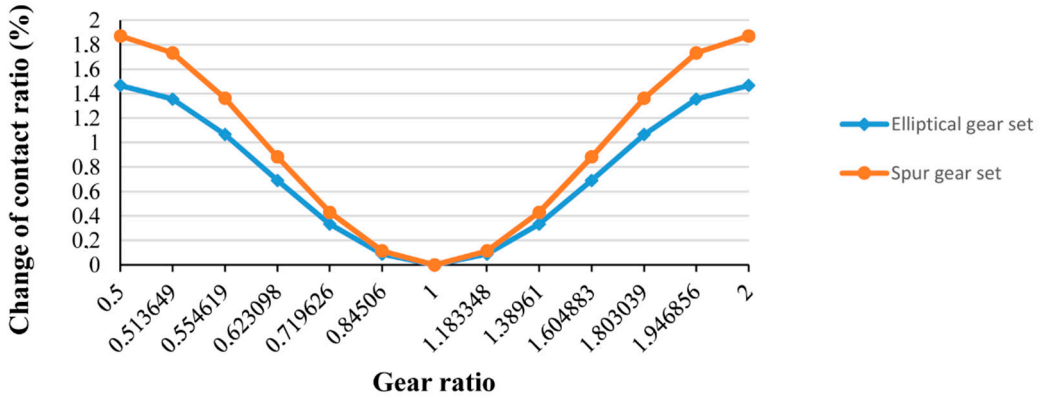


Figure 25. Comparison of the change of the contact ratio parameter.

Designed elliptical gearing has the greatest meshing line AE value for the teeth meshing pair which has a gear ratio u = 1.0. This elliptical gearing is characterized in that the gearing is composed of teeth whose profiles are not the same shape. Therefore, the length of the meshing line *AE* and contact ratio are not constant for each pair of teeth in meshing, as in a standard circular spur gear.

In Figure 26, the velocity diagram for intermeshing teeth 4 (driving gear) and 8 (driven gear) in the central point of mesh is shown.

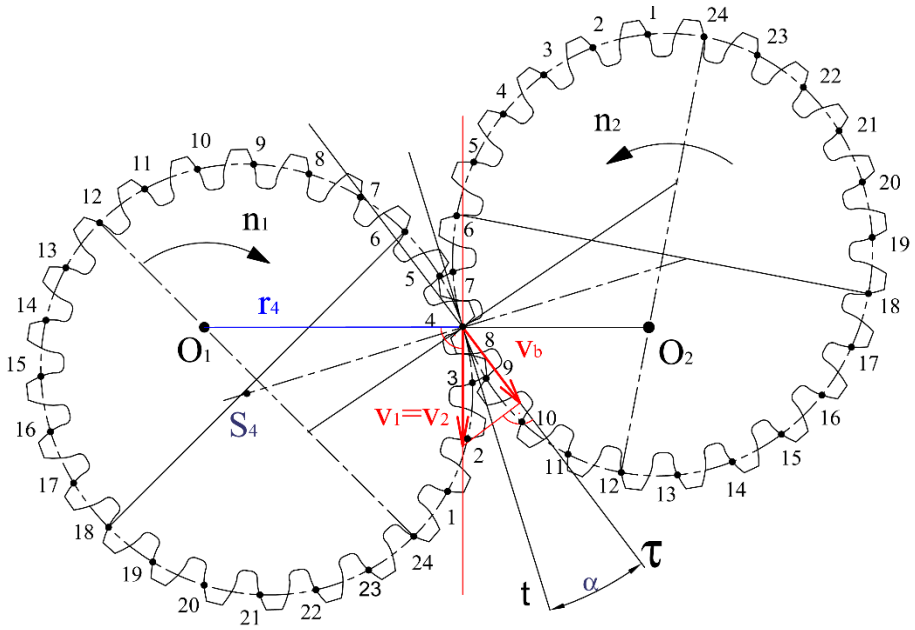


Figure 26. Velocity relations for the intermeshing teeth 4 and 8 in the central point of mesh.

For the designed elliptical gear set, the magnitude of the circumferential velocity in the central point of mesh is different for each intermeshing pair of teeth. The direction of circumferential velocities of individual pairs of intermeshing teeth is identical, their position between the centers of rotation changes (Figure 27).

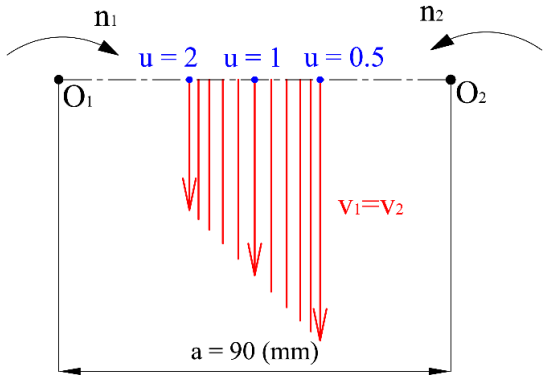


Figure 27. Change of the magnitude and the position of the circumferential velocity in central points of mesh of teeth pairs.

In Figure 28, the change of the circumferential velocity magnitudes in the central points of mesh for individual intermeshing pairs of teeth at one revolution of the elliptical gears is shown.

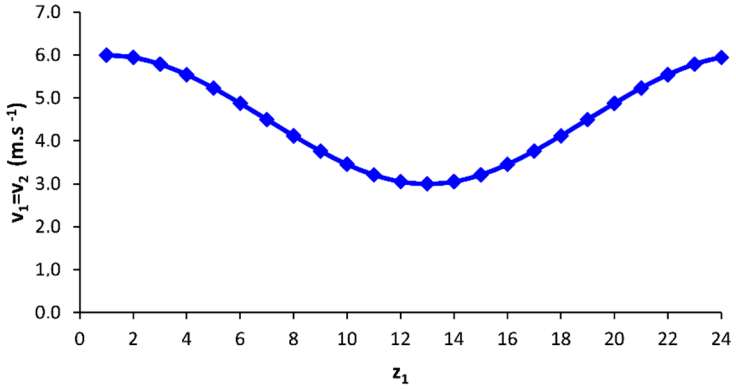


Figure 28. Circumferential velocities in the central point of mesh of teeth pairs.

The circumferential velocity in the central points of mesh of individual intermeshing pairs of teeth is not constant, but it changes continuously depending on the changing gear ratio.

3.4. Verification of the Correctness of the Design of Elliptical Gearing

The correctness of the gear meshing was verified using 3D contact analysis of the teeth by SolidWorlds. A motion analysis was performed here. Motion simulation provides complete, quantitative information about the kinematics (for example about position, velocity, acceleration, etc.). Everything needed to perform motion simulation has been defined in the CAD assembly mode. In the case of this elliptical gear set, it was necessary to define the input angular velocity, the monitored points and the result of the motion in the motion simulation program. Some information from the research work [39] was also used in the kinematic analysis. The result was an examination of tooth collisions during gearing meshing. Based on this analysis, there is no collision of teeth during gearing meshing. The angular velocity was also verified. In Figure 29 on the left is the course of angular velocities for the driving wheel and on the right for the driven wheel obtained by SolidWorks motion analysis.

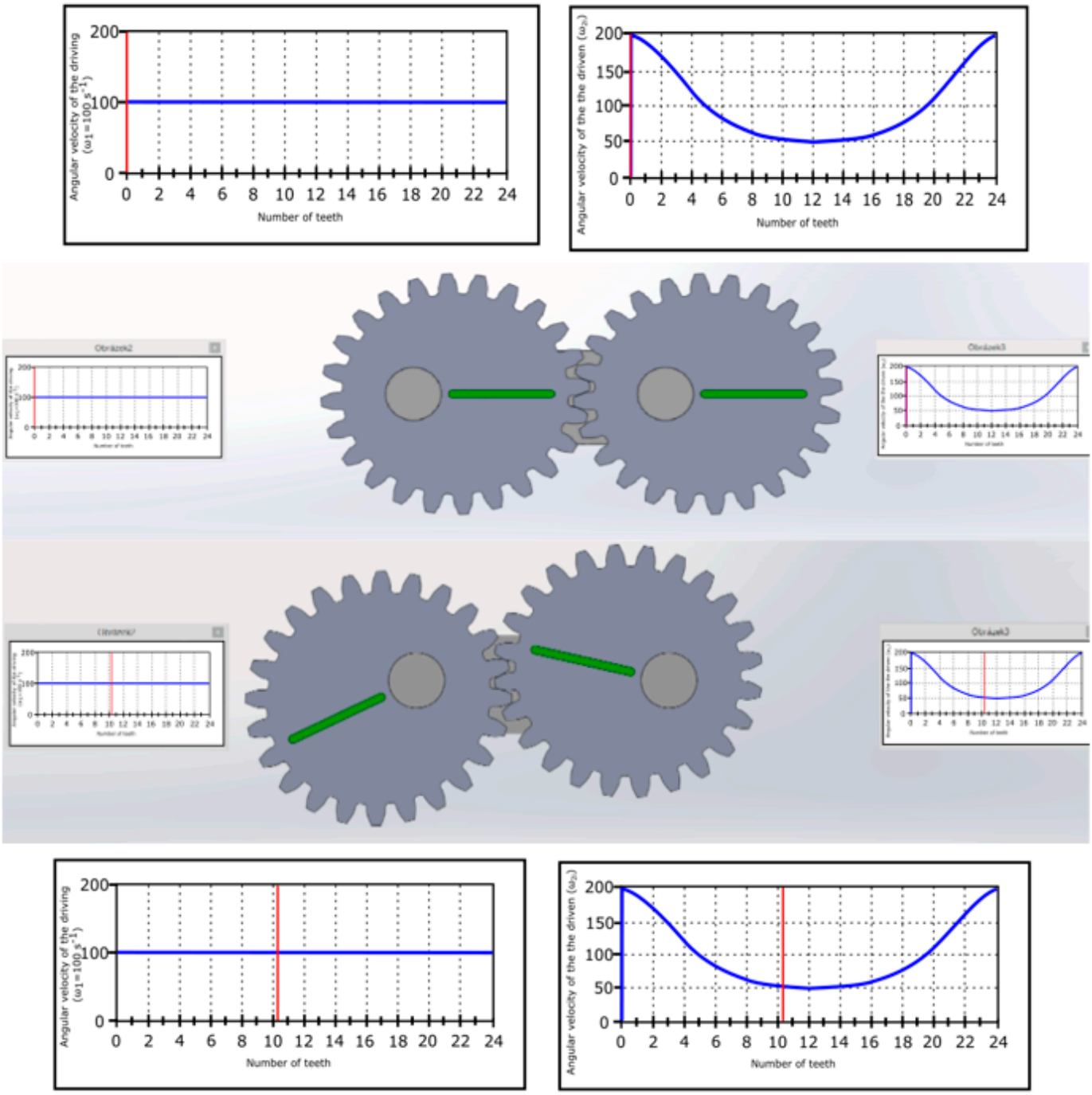


Figure 29. Motion analysis by SolidWorks.

The designed non-circular wheels were printed as 3D models (Figure 30). The geometric model of the elliptical wheel also served as a basis for production. Elliptical gears were made on an NC machine for electrospark cutting. An NC machine for electrospark cutting (so-called wire cutter) EIR 005 B with RS-ER5 control was used for production. Its accuracy is 0.01 mm and roughness Ra 1.6 μm. The wheels were tested by the customer and met all his requirements.

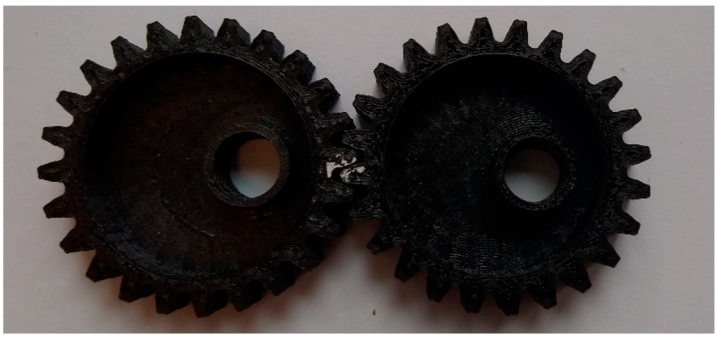


Figure 30. 3D printing of a designed elliptical gear.

4. Conclusions

Gear transmissions with a continuously changing gear ratio are finding more and more applications in practice. A suitable design of the pitch curve shape for the required range of the changing gear ratio is the first crucial step for the successful solution of a problem. For the required continuously changing gear ratio, the elliptical shape of the pitch curve was designed. The gear set was designed as a pair of identical elliptical gears. The center of rotation is in one of the foci of the pitch ellipse, they are eccentrically placed elliptical gears. The active curve of the tooth profiles is an involute and it is different for the active and passive side of a tooth. These are gears with an asymmetrical tooth profile. Unlike the involute portion of teeth profiles of "standard" circular gears, where the evolute of the involute is the base circle, in this case the evolute of the involute is the ellipse. Each of the twelve teeth of the gear is different and the other twelve teeth of the same gear are the same.

The gear ratio of the designed elliptical gear set is not constant, but is continuously changing in the range from 0.5 through 1.0 to 2.0 and back. This is how the gear ratio varies during one revolution.

Unlike standard circular gears, where the angular speed of the driving and also of the driven gear is constant, in this case, the angular velocity of the driven eccentrically placed gear is not constant, but it varies depending on the continuously changing gear ratio.

In the case of the designed elliptical gear set, the magnitude of the circumferential velocity in the central point of mesh is different for each intermeshing pair of teeth. The direction of circumferential velocities of individual pairs of intermeshing teeth is identical, their position between the centers of rotation changes.

In further research, the authors plan to deal with the problem of the deformation and stiffness of the created gearing. The deformation of the designed elliptical, eccentrically placed gear set differs from the deformation of a standard gearing. The overall course of the deformation changes during the mesh and it is different for each pair of intermeshing teeth.

Author Contributions: Conceptualization, S.M.; methodology, S.M. and G.F.; investigation, S.M. and M.U.; data analysis, S.M. and S.S.; writing—original draft preparation, S.M. and V.M.; writing—review and editing, M.U., G.F. and V.M. All authors have read and agreed to the published version of the manuscript.

Funding: This work is a part of these projects VEGA 1/0403/18, VEGA 1/0600/20, VEGA 1/0528/20, KEGA 012TUKE-4/2019, KEGA 013TUKE-4/2019, APVV SK-SRB-18-0053.

Conflicts of Interest: The authors declare no conflict of interest.

References

1. Lewis, M. Gearing in the ancient world. *Endeavour* **1993**, *17*, 110–115. [CrossRef]
2. Zarebski, I.; Sałacinski, T. Designing of non-circular gears. *Arch. Mech. Eng.* **2008**, *LV.*, 275–292.
3. Mundo, D. Geometric design of a planetary gear train with non-circular gears. *Mech. Mach. Theory* **2006**, *41*, 456–472. [CrossRef]

4. Marimuthu, P.; Muthuveerappan, G. Design of asymmetric normal contact ratio spur gear drive through direct design to enhance the load carrying capacity. *Mech. Mach. Theory* **2016**, *95*, 22–34. [CrossRef]
5. Chen, Y.-Z.; Huang, H.; Lv, Y. A variable-ratio line gear mechanism. *Mech. Mach. Theory* **2016**, *98*, 151–163. [CrossRef]
6. Kowalczyk, L.; Urbanek, S. The geometry and kinematics of a toothed gear of variable motion. *Fibres Text. East. Eur.* **2003**, *11*, 60–62.
7. Schmidt, M. Window shade with a shade panel. U.S. Patent 6,672,363, 6 January 2004.
8. Litvin, F.L.; Gonzalez-Perez, I.; Fuentes, A.; Hayasaka, K. Design and investigation of gear drives with non-circular gears applied for speed variation and generation of functions. *Comput. Methods Appl. Mech. Eng.* **2008**, *197*, 3783–3802. [CrossRef]
9. Lin, C.; Hou, Y.; Gong, H.; Liu, G.; Li, L. Design and analysis of transmission mode for high-order deformed elliptic bevel gears. *Jixie Gongcheng Xuebao (Chin. J. Mech. Eng.)* **2011**, *47*, 131–139. [CrossRef]
10. Liu, D.; Ren, T.; Jin, X. Geometrical model and tooth analysis of undulating face gear. *Mech. Mach. Theory* **2015**, *86*, 140–155. [CrossRef]
11. Bair, B.-W. Computer aided design of elliptical gears with circular-arc teeth. *Mech. Mach. Theory* **2004**, *39*, 153–168. [CrossRef]
12. Okada, M.; Takeda, Y. Optimal design of nonlinear profile of gear ratio using non-circular gear for jumping robot. In Proceedings of the 2012 IEEE International Conference on Robotics and Automation, Saint Paul, MN, USA, 14–18 May 2012; pp. 1958–1963.
13. Zhuang, W.; Hua, L.; Han, X.; Zheng, F. Design and hot forging manufacturing of non-circular spur bevel gear. *Int. J. Mech. Sci.* **2017**, *133*, 129–146. [CrossRef]
14. Zheng, F.; Han, X.; Hua, L.; Zhang, M.; Zhang, W. Design and manufacture of new type of non-circular cylindrical gear generated by face-milling method. *Mech. Mach. Theory* **2018**, *122*, 326–346. [CrossRef]
15. Shi, K.; Yao, Y.-A.; Lin, S. Design Method for N-Lobed Noncircular Bevel Gears. *Adv. Mech. Eng.* **2020**, *12*, 1687814019897498. [CrossRef]
16. Yu, Y.; Liu, J.; Ye, B.; Yu, G.; Jin, X.; Sun, L.; Tong, J. Design and Experimental Research on Seedling Pick-Up Mechanism of Planetary Gear Train with Combined Non-circular Gear Transmission. *Chin. J. Mech. Eng.* **2019**, *32*, 49. [CrossRef]
17. Li, M.; Shi, T.; Yang, J.; Qi, L.; Zhao, Z. Realizing nonlinear springs through noncircular planetary gears. *Mech. Mach. Theory* **2021**, *156*, 104151. [CrossRef]
18. Hou, Y.; Lin, C. Kinematic analysis and experimental verification of an oval noncircular bevel gears with rotational and axial translational motions. *J. Braz. Soc. Mech. Sci. Eng.* **2019**, *42*, 60. [CrossRef]
19. Prikhodko, A. Experimental kinematic analysis of an intermittent motion planetary mechanism with elliptical gears. *J. Meas. Eng.* **2020**, *8*, 122–131. [CrossRef]
20. Sałaciński, T.; Przesmycki, A.; Chmielewski, T. Technological Aspects in Manufacturing of Non-Circular Gears. *Appl. Sci.* **2020**, *10*, 3420. [CrossRef]
21. Radzevich, S.P. *Dudley's Handbook of Practical Gear Design and Manufacture*; CRC Press: Boca Raton, FL, USA, 2012.
22. Nemcek, M.; Dejl, Z. New method of a calculation of equidistant coordinates of an involute tooth profile for FEM calcula-tions of gears. In Proceedings of the ASME Design Engineering Technical Conference, San Diego, CA, USA, August 30–September 2 2009.
23. Medvecká-Beňová, S. Meshing Condition and Kinematic Properties of non-circular Gear. *Acta Mech. Slovaca* **2016**, *20*, 16–21. [CrossRef]
24. Tsai, S.-J.; Huang, G.-L.; Ye, S.-Y. Gear meshing analysis of planetary gear sets with a floating sun gear. *Mech. Mach. Theory* **2015**, *84*, 145–163. [CrossRef]
25. Šalamoun, Č.; Suchý, M. *Čelní a Šroubová souKolí s Evolventním Ozubením*; SNTL: Praha, Slovakia, 1990.
26. Laczik, B. Involute Profile of Non-Circular Gears. *Inst. Mech. Eng. Coll. Dunaújváros* **2004**, *8*, 1–5.
27. Liu, D.; Ren, T. Creating pitch curve of closed noncircular gear by compensation method. *Jixie Gongcheng Xuebao (Chin. J. Mech. Eng.)* **2011**, *47*, 147–152. [CrossRef]
28. Figlus, T.; Koziol, M.; Kuczynski, L. No Ti the Effect of Selected Operational Factors on the Vibroactivity of Upper Gearbox Housings Made of Composite Materials. *Sensors* **2019**, *19*, 4240. [CrossRef] [PubMed]
29. Maláková, S. Kinematic properties and mesching condition of elliptical gear train. *Sci. J. Sil. Univ. Technol. Transp.* **2019**, *104*, 95–105.
30. Dooner, D.B. *Kinematic Geometry of Gearing*; Wiley: Hoboken, NJ, USA, 2012; ISBN 9781119950943.
31. Meneses, J.; Garciaprada, J.C.; Castejon, C.; Rubio, H.; Abad, E.C. The kinematics of the rotary into helical gear transmission. *Mech. Mach. Theory* **2017**, *108*, 110–122. [CrossRef]
32. Bair, B.-W. Computer aided design of non-standard elliptical gear drives. *Proc. Inst. Mech. Eng. Part C J. Mech. Eng. Sci.* **2001**, *216*, 473–482. [CrossRef]
33. Kosters, M. Curvature-dependent parameterization of curves and surfaces. *Comput. Des.* **1991**, *23*, 569–578. [CrossRef]
34. Schubert, P.; Kirchner, M. Ellipse area calculations and their applicability in posturography. *Gait Posture* **2014**, *39*, 518–522. [CrossRef]
35. Tsay, C.-B.; Liu, W.-Y.; Chen, Y.-C. Spur gear generation by shaper cutters. *J. Mater. Process. Technol.* **2000**, *104*, 271–279. [CrossRef]
36. Figliolini, G.; Angeles, J. The Synthesis of Elliptical Gears Generated by Shaper-Cutters. *J. Mech. Des.* **2003**, *125*, 793–801. [CrossRef]
37. Litvin, F.L.; Lian, Q.; Kapelevich, A.L. Asymmetric modified spur gear drives: Reduction of noise, localization of contact, simulation of meshing and stress analysis. *Comput. Methods Appl. Mech. Eng.* **2000**, *188*, 363–390. [CrossRef]

38. Slovak National Standard STN 01 4686 Strength Calculation of Gears. 1975. Available online: http://www.visitsingapore.com/en_au/editorials/singapore-off-the-beaten-track-neighborhoods.html (accessed on 20 November 2017).
39. Xia, L.; Li, D.Z.; Han, J. Research on Mathematical Modeling and Kinematic Simulation of Elliptic Family Gears. In *Key Engineering Materials*; Trans Tech Publications Ltd.: Freienbach, Switzerland, 2013; pp. 300–304. [CrossRef]